Electrochimica Acta 311 (2019) 211–220

Contents lists available at ScienceDirect

Electrochimica Acta

journal homepage: www.elsevier.com/locate/electacta

Ageing mechanisms in electrochemical capacitors with aqueous redox-active electrolytes

Anetta Platek [1], Justyna Piwek [1], Krzysztof Fic[*,1], Elzbieta Frackowiak[**,1]

Poznan University of Technology, Institute of Chemistry and Technical Electrochemistry, Berdychowo 4, 60-965, Poznan, Poland

ARTICLE INFO

Article history:
Received 20 January 2019
Received in revised form
17 April 2019
Accepted 18 April 2019
Available online 25 April 2019

Keywords:
Redox active electrolyte
Aqueous electrolyte
Carbon electrodes
Galvanostatic cycling test
Floating test
Potassium iodide

ABSTRACT

This paper reports on the long-term performance of electrochemical capacitor operating in 1 mol·L^{-1} KI solution subjected to two ageing protocols, i.e., galvanostatic *cycling* and potentiostatic *floating*. Ageing tests have been performed at similar voltage conditions (1.5 V), estimated from the coulombic and energetic efficiency as well as the self-discharge analysis. The end-of-life criterion (80% of initial capacitance retained) was the same for both procedures. The influence of the ageing methodology on the structural and textural changes in electrode material has been discussed. The results obtained allowed for failure mechanisms description in the *floating* tests in comparison to traditional galvanostatic *cycling*. It has been stated that *de facto* the structural changes do not diminish the long-time performance. Notwithstanding, it has been found that galvanostatic *cycling* has a definitely stronger and detrimental impact on the carbon structure. Interestingly, both ageing methodologies affect the electrode porosity in a similar way. The nitrogen adsorption measurements indicated that the specific surface area decrease correlates with the capacitance fade. Changes observed in the pore size distribution allowed us to conclude that the porosity of both electrodes is blocked by adsorbed and/or deposited species. It looks that *floating* causes higher pore clogging especially for positive electrode.

1. Introduction

Recent development in electrochemical capacitors is oriented towards the improvement of their gravimetric (or volumetric) energy and power [1,2]. Certainly, the goal is to retain their high power response at increased energy output as they would compete with traditional battery systems like Li-ion or Ni-MH [3–5]. In order to increase the amount of energy stored in the system, two approaches could be followed: boosting the specific capacity by the faradaic contribution from redox species or extending the voltage window of the device [6–11]. Such procedures are governed by equation (I) for symmetric ECs [12,13]

$$E_{max} = \frac{1}{2} \cdot C \cdot {U_{max}}^2 \quad \text{(I)}$$

describing the relation between the specific energy (E), capacitance (C) and max. voltage of the system. The specific capacitance depends on the electrode material, its porosity, and specific surface area. Unless the faradaic contribution is not the case, the capacitance of electric double-layer varies between 10 and 50 μF·cm^{-2}, therefore, one can expect linear dependence of capacitance value with the surface of the electrode [1,14–17]. Taking into account the properties of the activated carbons, being the most often applied electrode materials, the gravimetric capacitance does not exceed 150–200 F·g^{-1}.

Fortunately, the electrolyte-side approach appears to be much more prospective [18–22]. All electrochemical capacitors could be classified into one of three groups by the type of electrolyte used: aqueous [22,23], organic [24] or ionic-liquid-based [25,26]. When using organic medium, the max. voltage is relatively high (>2.5 V) despite the detrimental effect of electrode sub-microporosity [27]. However, their specific capacitance is restricted to 50–100 F·g^{-1} (expressed per single electrode mass) and due to the limited conductivity of the electrolytic medium (<20 mS·cm^{-1}), their power rate is somehow moderate [28]. Moreover, usually flammable and toxic solvents, such as acetonitrile or propylene carbonate, raise the issue of user safety and negative environmental impact. Therefore,

* Corresponding author.
** Corresponding author.
E-mail addresses: krzysztof.fic@put.poznan.pl (K. Fic), elzbieta.frackowiak@put.poznan.pl (E. Frackowiak).
[1] All authors are ISE members.

https://doi.org/10.1016/j.electacta.2019.04.117

scientific attention has been attracted by the aqueous electrolytes and their application in electrochemical capacitors [29]. The conductivity of water-based medium (>50 mS·cm^{-1}) ensures the excellent charge propagation and high specific capacitance values (100–200 F · g^{-1}) retained even at high current densities [30]. Nonetheless, because of the 'narrow' electrochemical stability of water, their operational voltage window is by principle limited to 1.23 V. The corrosion of current collectors and internal resistance increase issues cannot be also neglected [31]. Interestingly, the electrolyte pH can substantially impact the max. voltage. At high operating voltages, the electrolyte is always being decomposed, thus, hydrogen and oxygen are produced. These products react with all cell components and it must result in performance fade and makes the lifetime shorter. Obviously, at low pH values, the corrosion process is prone to occur. Although, when noble metal current collectors are applied (i.e., gold), this process is partially inhibited. However, the application of noble metals influences the overall price, therefore, stainless steel has been proposed as an optimal current collector material.

For all these reasons, water-based solutions of the neutral salts, i.e., Li_2SO_4 or $LiNO_3$, emerged recently as high-voltage aqueous electrolytes [32–40]. Their neutral pH allows the voltage window to be extended. Increase in their electrochemical stability on porous electrodes might be explained by the local pH changes (i.e., in micropores of activated carbon). In such a case, the local overpotentials improve the overall stability of the electrolyte even up to 1.6 V. In order to prove that the system is really capable to operate at the voltage claimed, various ageing (or long-term) tests should be performed [41–50]. Initially, the galvanostatic *cycling* procedure was reported. This methodology suggests a sequence of repeated charging/discharging cycles even up to 1 000 000 times. It was believed that high current regimes should be used (1 or 2 A· g^{-1}) in order to imitate the harmful conditions for the system. Today it is known that the advantages of such test might be debatable. Once high current regime is applied (10 A· g^{-1}), it is impossible to discuss on the stability of the system because charging/discharging process is too fast and parasitic side reactions are inhibited. The ions are capable neither of penetrating the pores nor of returning to the electrolyte bulk. Furthermore, the ohmic drop at high current loads is usually remarkable and cannot be neglected. Given that, one might assume that the 'real' ageing process is different. On the other hand, testing at soft regimes could lead to misleading results likewise, especially for redox-based systems. It has been found that mild current loads might promote the reduction and oxidation processes at the electrolyte/electrode interface (at respective potentials). Apparently, no universal set of parameters for electrochemical capacitor ageing controlled by galvanostatic *cycling* has been proposed yet [51].

Being on-duty, the capacitors are very often charged quickly and immediately discharged; however, it never happens up to 1 000 000 times at once. Additionally, the time required to perform such a procedure is very long, usually counted in months. Therefore, another ageing protocol called *floating* (or voltage-holding test) has been proposed [46]. It might be considered as an accelerated ageing procedure. However, the principle of this technique cannot be directly compared with typical *cyclability* tests done with galvanostatic charging/discharging. In fact, the *floating* protocol includes a set of steps to be followed: the first one is a galvanostatic charging of the system with the required current density until certain voltage (U_{max}). Then, the voltage is retained usually for 2 h or at least until the leakage current is stable. Then, the system is discharged in galvanostatic mode and thus the specific capacitance of the charging/discharging process might be measured. At a first glance, there is no doubt that the *floating* protocol is more harmful to the capacitors than the galvanostatic cycling. At least the exposure time at high voltages is much longer than for *cycling*. This suggests that the processes triggered are of different origin and there are several possible reasons for performance fade.

In fact, there is no direct answer whether the *cycling* or *floating* protocol is 'better' or closer to the real ageing of the system. It seems that only the comparison of both techniques might bring an insightful, reliable result. Nonetheless, besides the comparison of *cycling* and *floating*, the explanation of mechanisms occurring during both techniques for aqueous systems is still missing. Therefore, several questions require to be answered: what is the criterion of the *floating* test which could be comparable with 1 000 000 cycles? Does the current density used during charging the capacitor to the required voltage influence the ageing mechanisms? Why usually only 100 h of *the floating* test are shown in the papers?

Undoubtedly, there is no direct answer to these questions. Therefore, this problem became the point of our interest. How to do – and are we allowed for – a fair comparison of both techniques? What is the safety limit that matters? Do the conditions of different ageing tests influence the final outcome of the measurement?

Our motivation for this research was to bring an insight into ageing mechanisms in aqueous, redox-based electrochemical capacitors. We are aware that the subject to be covered is very broad, and many factors need to be carefully considered. For that reason, we have divided our work into the parts.

In various papers, one can find a claim that the energy of the electrochemical capacitors is moderate (if compared to the batteries). In order to enhance the energy output, the implementation of faradaic contribution is necessary. Although several solid-state materials (based on transition metal oxides such as MnO_2 or RuO_2) have been proposed as 'pseudocapacitance' source [10,19,52–57], the concept of redox-active electrolytes offers many advantages – improved diffusion in the liquids state, adjustable redox potentials (by pH and concentration) and commercial feasibility [58–61]. The aqueous solution of iodides (1 mol L^{-1}) has been proposed as a source of high capacitance for carbon-based electrochemical capacitors, owing to their redox activity ($I_2/2I^-$) [62]. Despite revealing many advantages, the main drawback is the limited lifetime of the capacitors exploiting such electrolytic medium. It is worth highlighting that iodides have also been extensively studied in various configurations, either in aqueous solutions [63], as an additive to other electrolytes [22,64] (including organic ones) or as a carbon surface modifier. Iodine redox activity is usually observed on the positive electrode, where the following redox reaction occurs:

$$2I^- \leftrightarrow I_2 + 2e^- \quad (1)$$

According to the Pourbaix diagram, besides the reaction (1), other processes may simultaneously occur, as they depend on the pH of the solution:

$$I^- + I_2 \leftrightarrow {I_3}^- \quad (2)$$

$$2{I_3}^- \leftrightarrow 3I_2 + 2e^- \quad (3)$$

$$3I_2 + 6OH^- \leftrightarrow 5I^- + {IO_3}^- + 3H_2O \quad (4)$$

$$2{I_3}^- + 3H_2O \leftrightarrow 5I^- + {IO_3}^- + 6H^+ \quad (5)$$

Several *operando* studies confirmed, that the redox activity of iodine on carbon electrode provokes the surface functionality changes and affects the overall performance [61,63,65,66]. Furthermore, the concentration and kind of the iodine-based species at the interface changes in time – at elevated potentials

polyiodides (I_3^-, I_5^- and I_7^-) are most likely formed. Therefore, it is essential to study the long-term behaviour, as their exceptional features may be diminished in time. It has been already stated that (poly)iodides might be confined into the porosity of the positive electrode [66]. They can be also 'activated' during electrochemical *cycling*; that results in the 'increase' of specific capacitance [67] but shortly after the performance fades very quickly. This suggests that the mechanisms might be really different. We believe that the improvement of the long-term performance comes from deep understanding of the ongoing processes. For that reason, we provide a comprehensive electrochemical study on this topic supported by physicochemical investigations.

2. Experimental

Symmetric electrochemical capacitors with stainless steel 316L current collectors have been assembled with carbon cloth electrodes KYNOL 507-20 (10 mm diameter, the mass of ca. 9.5 mg). The material has been selected as a self-standing electrode, in order to eliminate the detrimental influence of binder on the electrode porosity [68]. Whatman GF/A glass fibre with a diameter of 12 mm and thickness 260 μm played a role of the separator. Laboratory scale system Swagelok® consists of Teflon® body cell, 2 small and 2 big gaskets and 2 caps. Potassium iodide provided by Sigma-Aldrich (ACS grade) served for preparation of 1 mol·L^{-1} solutions. The solutions were prepared shortly before the experiments and were colourless. All measurements have been conducted in properly sealed Swagelok® cells. Moreover, during disassembling of the cells, wet electrodes were taken out from the systems.

For the hybrid capacitor, 1 mol L^{-1} aqueous solution of KI (prepared as described above) has been used for the positive electrode. For the negative electrode, 0.5 mol L^{-1} aqueous solution of K_2SO_4 (Sigma-Aldrich, ACS grade) has been prepared. The electrodes were soaked with appropriate electrolytes, separated by Nafion® 117 (Sigma-Aldrich) membrane and assembled in the Swagelok® cell.

Physico-chemical analyses of both carbon material (porosity and structure) and electrolyte (pH and conductivity) have been performed prior to the electrochemical measurements. The systems were aged with two protocols: galvanostatic *cycling* and potentiostatic *floating*. Specific capacitance values have been controlled in time together with internal resistance and are expressed per mass of one electrode. After reaching 20% capacitance fade, the systems were disassembled. The carbon aged electrodes were cleaned with distilled water and n-hexane to remove the residue from electrolyte. Nitrogen adsorption/desorption was performed at 77 K (Micromeritics ASAP 2460). Calculations of the respective pore size distributions were done by 2D NL-DFT model with heterogeneous surface using SAIEUS programme from Jacek Jagiello [69–71]. Raman spectroscopy with 633 nm laser (DXR™ 2 Raman Microscope Thermoscientific) was carried out to monitor structure changes. The flow chart of experiments is presented in Fig. 1.

Fig. 2 represents the methodology of two ageing techniques used, i.e., *cycling* and *floating*. In order to qualitatively and quantitatively characterize the systems, cyclic voltammetry (denoted as CV), electrochemical impedance spectroscopy (EIS) and galvanostatic charging/discharging techniques have been used.

As one can see in Fig. 2, *the floating* procedure consists of more steps than *cycling*, because voltage holding test is followed by three full galvanostatic charging/discharging cycles. The current density used for charging the system up to the required voltage is the same as current density utilized in *cycling* measurements. In the *cycling* protocol, a set of 500 full galvanostatic charging/discharging cycles was conducted as one loop of the ageing procedure. In order to evaluate the qualitative performance, CV profiles within 0.0 ÷ 0.8 V and 0.0 ÷ 1.5 V voltage range have been recorded with the scan rate of 5 mV s^{-1}. EIS has been conducted in the frequency range 100 kHz–10 mHz at the capacitor voltage of 0 V, in order to keep the electrodes at the same potentials. Specific capacitance values have been calculated from each galvanostatic discharge curve (integral values). After reaching end-of-life criterion, i.e. 20% of initial capacitance loss, the systems were stopped, disassembled and analysed physicochemically.

3. Results and discussion

3.1. Determination of an operational voltage

Prior to the ageing procedures, fundamental electrochemical tests have been performed. In order to estimate the optimal operating conditions, the gradual extension of the voltage window in three-electrode set-up (two-electrode cell with the reference electrode) was done. Usually, the capacitors with iodide-solutions are claimed to work at the voltages up to 1.4 V [7,61,66,67,72–75]. However, as in the redox-based systems the applied voltage influences the electrochemical behaviour, the most 'harmful' conditions have been selected in order to evaluate the operation limits. Therefore, the capacitor voltage of 1.5 V, characterized by 90% of coulombic efficiency retention and energetic efficiency higher than 60% have been selected. The efficiency values were calculated from the galvanostatic charging/discharging process at a current load of 0.1 A·g^{-1}. Moreover, self-discharge (SD) of iodide-based ECs until 1.5 V is similar to the ECs with 1 mol·L^{-1} lithium sulphate, what leads to the conclusion that redox species are strongly attracted to the carbon surface. After exceeding 1.5 V the voltage drop is dramatically high for ECs with 1 mol·L^{-1} KI what proves, that this voltage is a maximal possible operational voltage window.

For 1.2 V capacitor voltage, normally claimed as a 'safe' limit, both coulombic and energetic efficiency values are higher than 90%. However, for the systems with iodides playing the role of redox-active additive, the operational voltage is very often higher than 1.2 V. For that reason, the cut-off voltage in our study has been selected to be equal to 1.5 V.

In Fig. 3A, cyclic voltammetry profiles recorded for a gradual cut-off voltage increase are presented. At 0.8 V, the curve is characterized by the redox-indicating shape and deviates from the typical rectangular profile. It can be seen that in the very narrow range of voltage (up to 1.0 V), pure electrostatic attractions play a major role in the charge accumulation process and are reflected in the rectangular shape of CV. Above 1.0 V, the specific capacitance is not linear along the voltage. This increase results from iodide/iodine redox activity. In galvanostatic charging/discharging profile (Fig. 3B) one can identify different charge storage mechanisms in electrodes. The positive electrode (red dashed line) operates in a very narrow potential range imposed by the redox activity of iodides ($I_2/2I^-$). Therefore, it is the so-called battery-type electrode. The negative electrode (blue dashed line) reflects typical electrostatic interactions - ions are electrostatically adsorbed and desorbed during charging/discharging process. However, for the full cell (black line) the redox contribution cannot be easily distinguished.

Besides, by comparison of the data represented in Fig. 3A and the profile in Fig. 3B, it may be also concluded that the current density influences the efficiency of charging/discharging process slightly: for 0.1 A·g^{-1} current load the coulombic efficiency was of 90%, while for 1 A·g^{-1} is at the level of 88%. Apart from the fact that it confirms very good charge propagation in iodide-based systems, it indicates that the current load does not play a significant role in performance fade (for the selected experiment conditions). Therefore, for the sake of time, 1 A·g^{-1} current density has been selected for the ageing tests with capacitor voltage of 1.5 V.

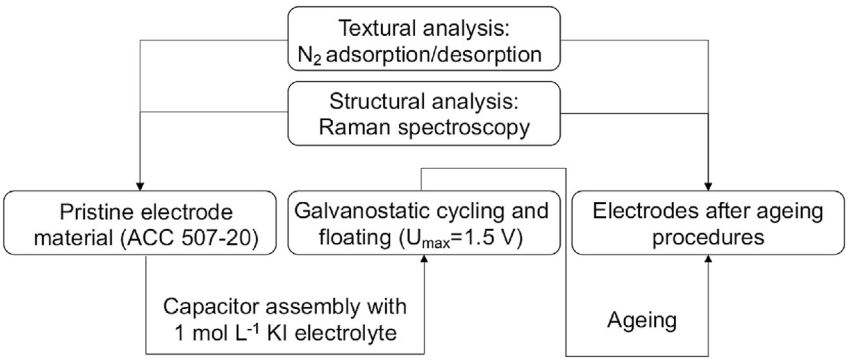

Fig. 1. Scheme of physicochemical analyses performed on electrode material after the ageing process.

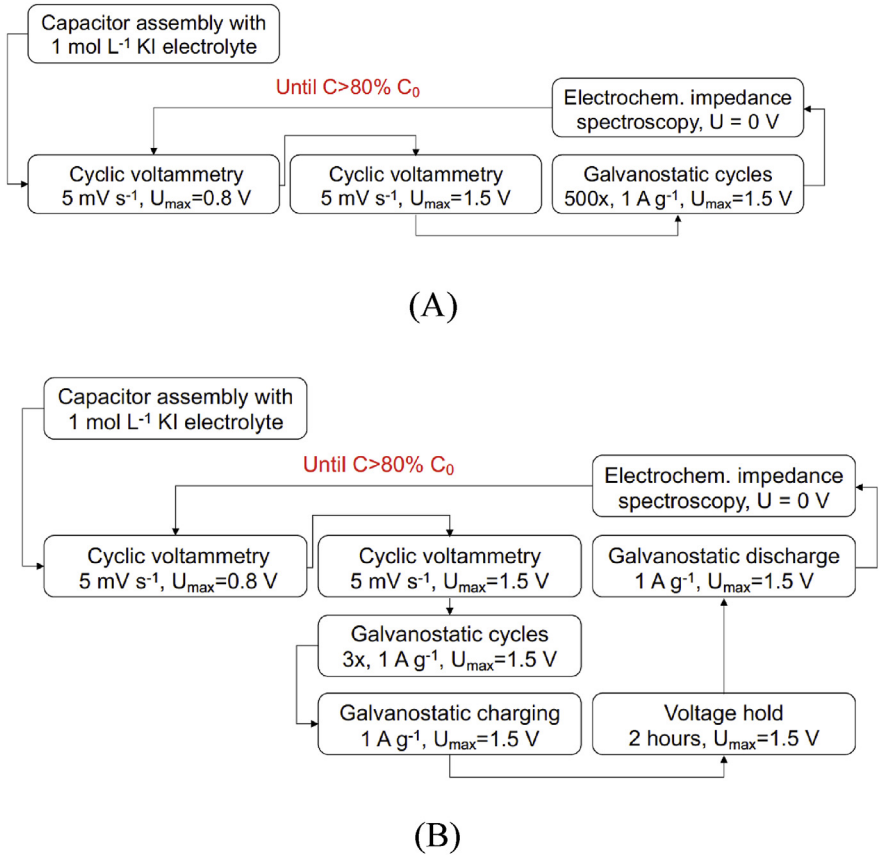

Fig. 2. Scheme of ageing protocols (A) galvanostatic *cycling* and (B) *floating*.

3.2. Floating and galvanostatic cycling tests

Electrochemical capacitors have been tested for long-term performance by two different methodologies described previously. The end-of-life criterion has been defined as 20% of initial capacitance loss.

For qualitative comparison of the effects coming from both ageing techniques, cyclic voltammetry curves (5 mV s^{-1}) have been recorded and are presented in Fig. 4A.

It could be noticed that CV profile recorded after *cycling* test (Fig. 4A) is characterized by very good charge propagation. Moreover, no qualitative change of redox activity is observed. This is not the case for the capacitor subjected to the *floating* test: the CV profile is ill-defined and reflects the strong change of capacitor performance (more resistive character). In this case, the system is exposed to long-term polarization at high maximum voltage where all parasitic reactions can take place. The redox activity has been shifted towards lower potential values and the corresponding peak is observed at the low capacitor voltages due to pH changes. This is in accordance with our previous remarks [58,72,73] and reflects the changes in the electrochemical processes ongoing in the system, reflected by the peaks appearing near 0 V (Fig. 4A). One can assume at least the following reasons for such a response. The major one is related to the redox activity of I^-/I_2 pair. It has been already noticed that pH of electrolytic solution shifts from neutral to slightly alkaline. Hence, the potential ranges of individual electrodes change and accordingly the redox activity of iodine/iodide couple shifts towards more negative values. Moreover, we cannot exclude the

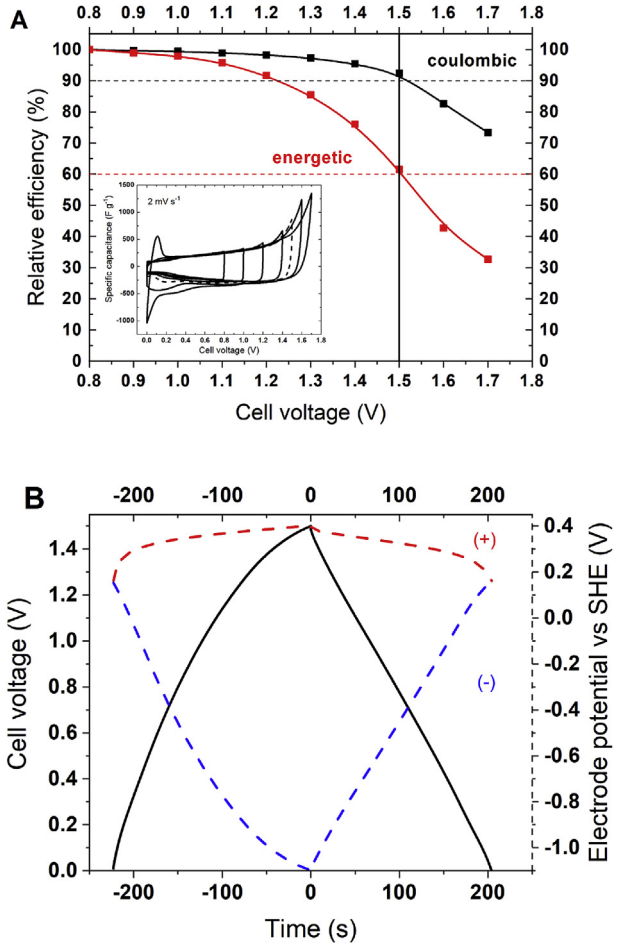

Fig. 3. Energetic and coulombic efficiency calculated from galvanostatic charging/discharging at 0.1 A·g^{-1} (A) with cyclic voltammetry profiles at 2 mV s^{-1} (inset) for capacitor operating with 1 mol·L^{-1} KI aqueous solutions; (B) galvanostatic (1 A·g^{-1}) profile for capacitor voltage 1.5 V and corresponding electrode profiles.

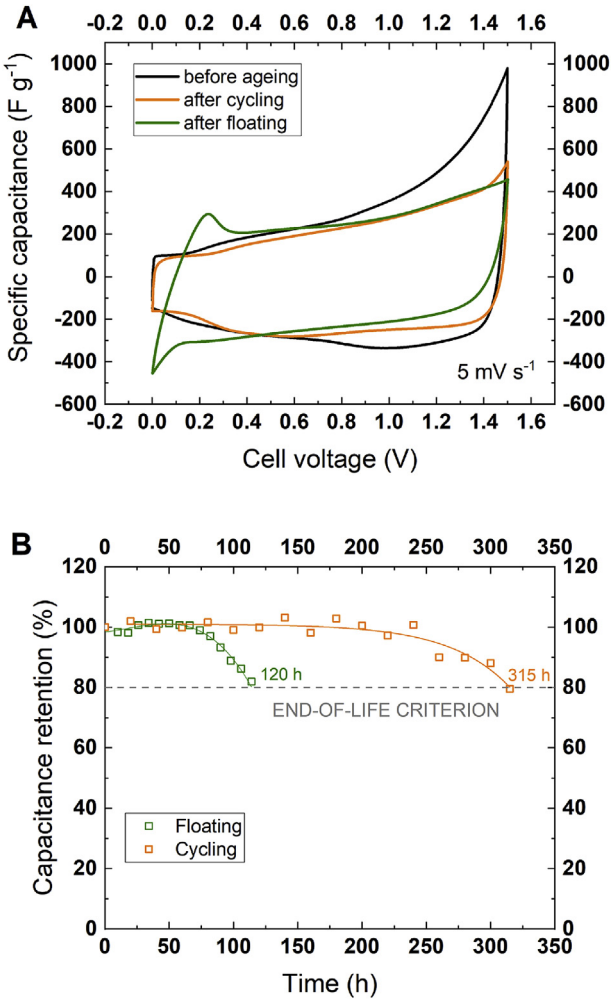

Fig. 4. Comparison of *floating* and *cycling* tests: A) cyclic voltammetry at scan rate 5 mV s^{-1} for fresh and aged systems; B) change of the relative capacitance vs. ageing time.

oxidation of carbon electrode into quinone/hydroquinone groups after long-term *floating* (proved by more resistive character). Such a redox couple gives the same electrochemical response [72]. Therefore, these two redox pairs should be considered. Additionally, hydrogen electrosorption on the negative electrode cannot be completely omitted taking into account that electrolyte turns into slightly alkaline. Hydrogen stored normally desorbs at low capacitor voltages (negative electrode potential near rest potential, E_0). Such peaks were observed for various aqueous electrolytes and have been confirmed by 3-electrode investigations [63].

Moreover, the capacitor subjected to the *floating* procedure demonstrates remarkably higher resistance. Thus, the qualitative comparison between those two ageing tests reveals noticeable differences between their mechanisms. Of course, the experiment time is different for *cycling* (315 h) and *floating* test (120 h) until the same result has been reached: 80% of capacitance. In Fig. 4B, the capacitance retention is shown *vs.* experiment time. Definitely, the *floating* is an accelerated ageing procedure in comparison to *cycling*. Furthermore, it seems that this test is less sensitive to the experimental conditions (e.g., temperature fluctuations) than the other techniques (CV and EIS) performed between the voltage hold steps. Since the capacitance values slightly increase between the voltage hold steps and galvanostatic *cycling* loops, it could be considered that cyclic voltammetry 'refreshes' the system. Such a 'self-healing' phenomenon indicates that some side-reactions might be reversible. However, taking the average of relative specific capacitance fluctuations, it could be seen that up to 240 h of operation it is ca. 100% retention, but after it starts to drop gradually. Thus, it can be concluded that *floating* is much more ageing-effective for the system as its operation time for reaching the same end-of-life criterion is almost 3 times shorter than in the case of *cycling*.

Besides the qualitative insight provided by cyclic voltammetry, a quantitative comparison was done. All the charge passing through the system separately during charging and discharging processes has been calculated from all electrochemical techniques performed according to the protocols (Fig. 5).

It is clear that during *floating* test much more charge is consumed during 'charging' (including voltage hold steps) than 'discharging'. It means that some charge is used for side reactions or electrolyte decomposition processes. As the resistance in the system increased, it has been assumed that this difference of charge results from the oxidation of the electrode material or formation of 'by-product' layer on it. This was confirmed by *post-mortem* analysis discussed later in the manuscript. Contrarily to the *floating* test, for the *cycling* procedure, the amount of charge is somehow equilibrated during charging and discharging processes. One should notice that an overall charge is twice higher than in the case of *the floating* experiment. Interestingly, this value is in accordance with the time ratio of both tests.

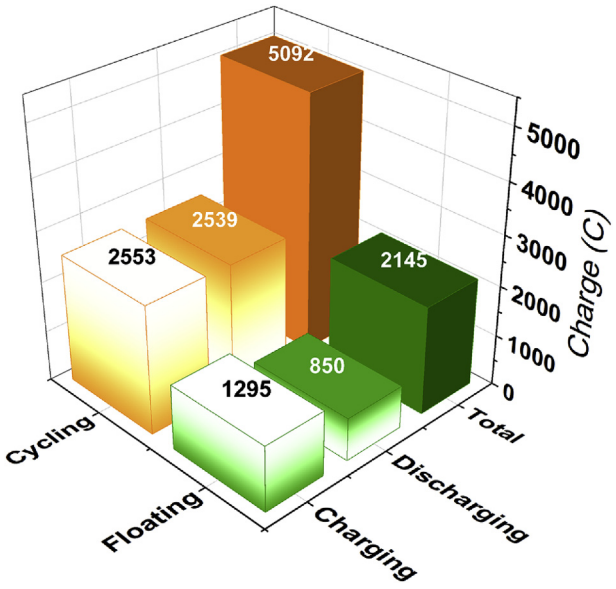

Fig. 5. Charge flowing through the system during *cycling* and *floating* protocols.

Since it was observed that *floating* induces some extra resistance in the system, electrochemical impedance spectroscopy has been performed. Fig. 6 presents the Nyquist plots recorded for the fresh system and for the systems subjected to ageing.

The capacitor before the ageing procedure is characterized by equivalent series resistance (ESR, measured at 100 kHz) of 0.42 Ohm. For the frequencies higher than equivalent distributed resistance (EDR), the curve resembles the characteristic profile for electrochemical capacitors based on porous activated carbon electrodes with well-visible diffusion contribution. The resistance of the cell subjected to the *galvanostatic cycling* procedure does not change significantly (as noticed on the voltammograms). The ESR slightly shifts to 0.53 Ohm, so only 25% increase is recorded. In the high frequency range, plots are overlapping but for the low frequency range, the profile deviates from the parallel position. This

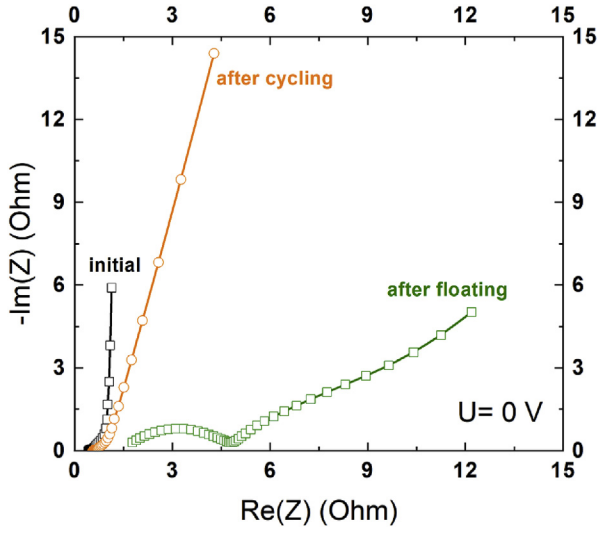

Fig. 6. Nyquist plots recorded for capacitors operating with 1 mol·L^{-1} KI solution before (black line) and after *cycling* (orange); *floating* (green). (For interpretation of the references to colour in this figure legend, the reader is referred to the Web version of this article.)

indicates that not only a pure electrostatic attraction occurs and definitely there is a redox contribution to the charge storage mechanism. The curve recorded after *the floating* experiment is definitely different. At a first glance, significant resistance increase is observed. ESR changed from 0.42 to 1.77 Ohm (320% increase). According to the International Standard IEC 62391-1:2015, an increase of 100% is a limiting factor of a lifetime of the electrochemical capacitor. Moreover, a large semicircle is observed, and the curve deflects. This indicates a performance failure which might have several reasons. Firstly, the oxidation of carbon electrode and incorporation of polyiodides into carbon matrix must be considered [61,63,66]. Polyiodides are not well dissolved in water, but KI solution is their good solvent, e.g., I_3^- solubility in KI is equal to 8 mol L^{-1}. However, amount of KI solution in the cell is limited, additionally KI is consumed for I_2 formation, hence, after long-term *cycling*, a solid-state deposit of polyiodides can precipitate. Presence of deposit on the aged electrodes was clearly proved by SEM images. Eventually, some deposits from the electrolyte-redox reactions (like KIO_3) might be considered [58,65]. It needs to be noticed that several iodine-based species can be involved in precipitation process. However, taking into account their solubility values in water at 25 °C: 112 g/100 mL (K_2CO_3), 9.16 g/100 mL (KIO_3), 0.42 g/100 mL (KIO_4) and 0.3 g/100 mL (I_2) only KIO_3 or KIO_4 can form a deposit. Nonetheless, according to the Pourbaix diagram IO_4^- creation requires extremely high potential what does not take place in a symmetric system. Additionally, during long-term performance, a bulk of the electrode tends to be strongly alkaline (pH ca. 11–12) what could trigger KIO_3 formation in the microporosity according to the Pourbaix diagram. Considering all the data, we assume that potassium polyiodides seem to be the main component of solid-state deposit but traces of mixed salts (iodate/carbonate) cannot be completely excluded. The final conclusion is that the *floating* is more harmful test than galvanostatic *cycling*.

3.3. *Post-mortem physico-chemical analysis of electrodes by N_2 adsorption/desorption and Raman spectroscopy*

After performing ageing measurements, a set of post-mortem physico-chemical analyses of electrode materials has been done (Fig. 7). In order to correlate the electrochemical changes with certain structural or textural differences, the results obtained for respective electrodes have been compared to the pristine carbon cloth. Firstly, nitrogen adsorption/desorption isotherms were collected in order to verify changes of the specific surface area S_{BET} (calculated by BET equation in the relative pressure range p/p_0 0.01–0.05 in the linearity region) and $S_{2D\text{-}NLDFT}$ as well as the pore size distribution modification.

A decrease in specific surface area is noticeable as indicated in Table 1 where S_{BET} and $S_{2D\text{-}NLDFT}$ are presented. It can be observed that $S_{BET} \gg S_{2D\text{-}NLDFT}$; however, trends between relative values are the same, being irrelevant to the calculation method applied. Therefore, both electrodes contribute to the ageing process. However, the differences between *cycling* and *floating* ageing are insignificant, especially for negative electrode.

To some extent, it was quite surprising since the iodides have been considered to affect positive electrode surface only. These results indicate that iodides (in their various forms) are most likely present on both electrodes. It seems that they block the access to the microporosity. This could result in a decrease of the specific surface area. Interestingly, both ageing tests diminish the surface in a similar manner considering pore size distribution. Therefore, the only decrease of the specific surface area influences the performance of the device during long-term analysis, and no decomposition reactions of aqueous electrolyte are expected to occur (hydrogen and oxygen evolution).

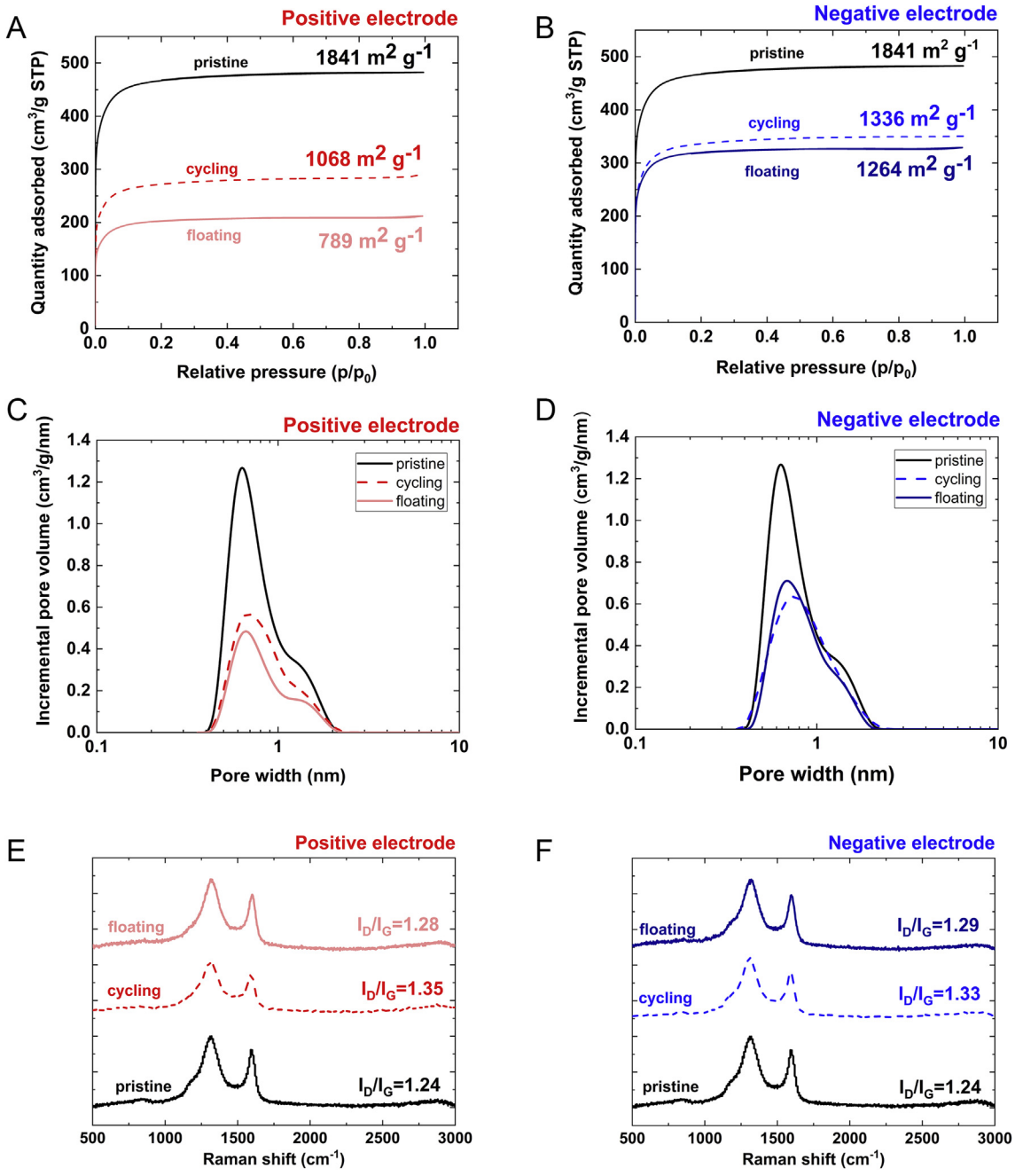

Fig. 7. Post-mortem physico-chemical analysis of electrode materials: A) and B) N_2 adsorption/desorption isotherms for positive and negative electrodes with S_{BET} values; C) and C) pore size distribution form 2D-NLDFT for both electrodes; E) and F) Raman spectra for both electrodes.

Table 1
Specific surface area calculated by BET or 2D-NLDFT method for pristine carbon cloth and electrodes after ageing.

	S_{BET} [$m^2 \cdot g^{-1}$]	Relative S_{BET} [%]	$S_{2D\text{-}NLDFT}$ [$m^2 \cdot g^{-1}$]	Relative $S_{2D\text{-}NLDFT}$ [%]
Pristine carbon	1841	100	1697	100
Positive electrode after *cycling*	1068	58	920	54
Negative electrode after *cycling*	1336	73	1120	66
Positive electrode after *floating*	789	43	692	41
Negative electrode after *floating*	1264	69	1083	64

For the positive electrode after the *floating* test, the calculated specific surface area is the lowest. It seems that ions are forced to penetrate the porous structure deeply and then they are trapped there. Since there is no reversed polarization (as for *cycling*), the porosity seems to be blocked irreversibly. For the negative electrodes, the isotherms obtained are almost overlapping each other. It

means that whatever the ageing method, some species block the porosity. Thus, it is assumed that iodides/polyiodides reveal the affinity not only to the positive electrode but generally to the carbon surface what needs to be considered in a symmetric device.

These findings are reflected in changed pore size distribution (PSD). Interestingly, the change is found only for the volume of pores, not their particular distribution. It can be seen that the maximum of PSD curves related to the average micropore diameter is located at the same points, with almost negligible shifts (also confirmed by Raman spectroscopy). Finally, the porosity analysis of the electrode material is in accordance with electrochemical data (20% of specific capacitance fade). However, the increase of resistance during the *floating* test could not be explained by this type of analysis.

In order to verify whether the ageing conditions cause the structural changes, the Raman spectra have been recorded. For the pristine carbon cloth, it is shown that I_D/I_G ratio is higher than 1. It provides information that such material is microporous with a high disorder degree. Structural changes do not vary between positive and negative electrodes remarkably. However, a noticeable difference could be observed when comparing electrodes after *cycling* and *floating* experiments. After long-term voltage hold, the electrode structure has been changed slightly as I_D/I_G ratio increased (Table 2). It results from increased intensity of 'disordered' peak (1350 cm^{-1}) and/or decrease the intensity of 'graphitic' peak (1580 cm^{-1}). It confirms the previous assumption that forcing the ions to penetrate the electrode deeply, changes the interlayer distance between graphene layers in the carbon matrix. Furthermore, a slight shift of D-band (ca. 3 cm^{-1}) might confirm that finding and support the PSD results, indicating a small shift in the pore size distribution. It seems that repeated adsorption and desorption of ions significantly modifies the structure of the carbon material. However, on the spectrum, it can be seen that the intensity of G peak decreases noticeably. It means that reversible ion fluxes (during *cycling*) affect the carbon structure much more than deep penetration enforced during *floating*.

Therefore, both ageing tests differ in governing mechanisms that might be correlated with different ion movements influencing the carbon structure. However, electrochemical fade corresponds to the porosity changes and this is the main reason for the performance deterioration.

3.4. Improvement of the long-term performance for the electrochemical capacitor with iodide-based electrolyte

As it has been stated that capacitance fade is correlated with decreasing of S_{BET} for both electrodes, the idea of blocking the iodide movement towards negative electrode appeared. Our motivation here was to 'protect' the negative electrode against the redox activity of iodides, which might occur when the system tries to equilibrate an enormous imbalance in the electrode potential ranges. Therefore, the concept of 'hybrid' system has been proposed: the electrolytes for the positive and the negative electrode have been separated by a selective, cation-exchange membrane. In such a case, only the cation is enabled to move between both electrodes. For this purpose, the 0.5 mol·L^{-1} solution of K_2SO_4 has been utilized as the electrolyte for the negative electrode. The concentration results from the solubility value of K_2SO_4 in water. Positive electrode operated in 1 mol·L^{-1} KI solution. Symmetric Swagelok® cells have been assembled and the same procedure for *the floating* test has been conducted. The first improvement is visible in the operation time (Fig. 8A).

After 120 h of *floating* test of the symmetrical systems, 80% of specific capacitance has been retained, while for the hybrid system still 87% has been found. It is almost 10% gained in comparison to the standard construction. Furthermore, after the same time of operation, no increase of internal resistance and deterioration of charge propagation is observed. Only the redox activity of $I_2/2I^-$ pair shifts towards lower voltage values, but it may be related with the *floating* mechanism. The main advantage of this hybrid concept is presented on the N_2 adsorption/desorption curves in Fig. 8B. It seems that for the symmetric cell, the negative electrode was affected by the iodide confinement, as the iodide-based species are supposed to be inactive on this electrode during capacitor operation. Therefore, the specific surface area decreased (from 1841 $m^2 \cdot g^{-1}$ to 1264 $m^2 \cdot g^{-1}$, i.e. 31% decrease), and the

Table 2
I_D/I_G ratio for pristine carbon cloth and electrodes subjected to ageing protocol.

	I_D/I_G
Pristine carbon	1.24
Positive electrode after *cycling*	1.35
Negative electrode after *cycling*	1.33
Positive electrode after *floating*	1.28
Negative electrode after *floating*	1.29

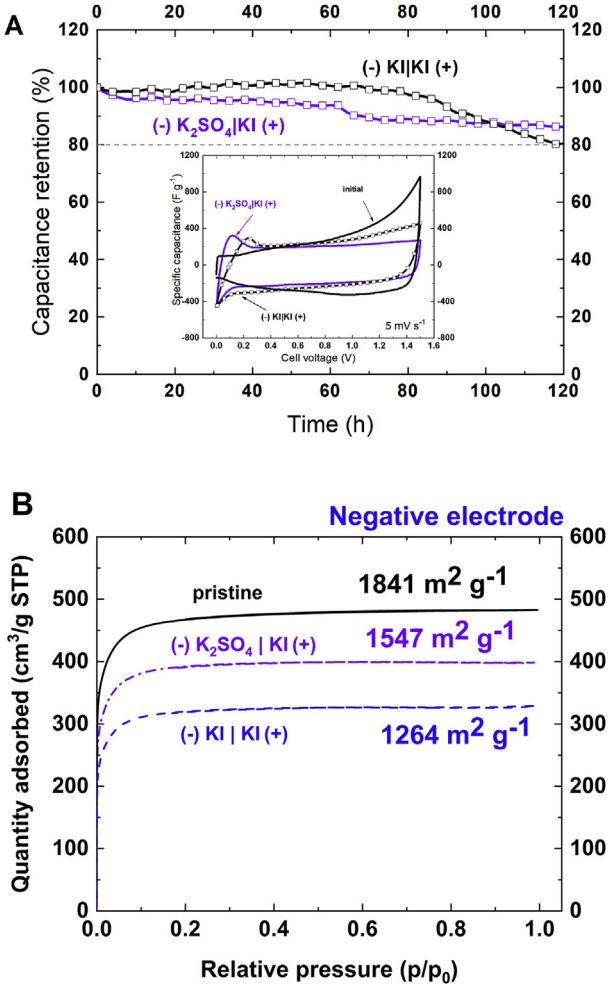

Fig. 8. Improvement of the long-term performance of redox based electrochemical capacitor: A) relative capacitance vs. time; inset: cyclic voltammograms at 5 mV s^{-1} for fresh system (plain black line), aged symmetric system (dashed blue line) and aged hybrid system (dashed violet line); B) N_2 adsorption/desorption isotherms for the negative electrodes with S_{BET} values. (For interpretation of the references to colour in this figure legend, the reader is referred to the Web version of this article.)

capacitance fade has been observed. After implementation of the cation-exchange membrane, blocking the iodide transfer to the negative electrode 'compartment', and different electrolyte for the negative electrode, the change of specific surface area is much smaller (from 1841 $m^2 \cdot g^{-1}$ to 1547 $m^2 \cdot g^{-1}$, i.e. 16% decrease). After 120 h operation of such a hybrid capacitor, the specific surface area is retained at 1550 $m^2 \cdot g^{-1}$, while it was 300 $m^2 \cdot g^{-1}$ less for the symmetric system. Therefore, blocking of specific surface area drop on the negative electrode improves overall performance of the electrochemical capacitor. This proves our statement concerning the reasons of performance for in ECs operating with 1 $mol \cdot L^{-1}$ KI. However, the cation-exchange membrane has not been designed especially for this purpose. Thus, we assume that applying various types of semi-permeable membranes would still improve the long-term performance. An implementation of the hybrid system is beneficial and does not significantly influence the specific capacitance of redox-based system.

4. Conclusions

The possible reasons for performance fade in electrochemical capacitors operating with redox-active electrolyte (1 $mol \cdot L^{-1}$ KI solution) have been identified and discussed. It has been shown that for such systems both ageing procedures, i.e., *cycling* or *floating*, impact in a different way the time of operation, structure of electrode and resistance of the total cell.

The *floating* test has been found to be more detrimental for the system, essentially by triggering the redox-based side-reactions and accelerating ageing of the system. It has been shown that the charge is consumed for side reactions and therefore, the resistance of the system increased. The origin is sought in the presence of polyiodide solid-state deposits blocking the access to the micropores. However, mixed salts iodates/carbonates cannot be completely excluded.

Cycling test takes longer time and does not influence the resistance of the cell remarkably. However, it has been found that the change of the carbon structure is more pronounced for this test. Here, the reason is sought in the ionic fluxes accessing and leaving the pores in the electrode bulk.

The specific capacitance fade is strictly correlated with specific surface area decrease. For both tests, similar S_{BET} and $S_{2D\text{-}NLDFT}$ changes have been observed for the same level of the capacitance fade.

Iodide/polyiodides anions hinder the access to the porosity on both, positive and negative, electrodes. Therefore, the improvement of the long-term performance is based on blocking iodides movement towards the negative electrode.

Acknowledgement

The authors would like to acknowledge the financial support from European Research Council received within the Starting Grant project IMMOCAP (GA 759603) under European Unions' Horizon 2020 research and innovation programme and from Preludium project financed by National Science Centre, Poland (project no. 2017/25/N/ST4/01738).

References

[1] F. Beguin, V. Presser, A. Balducci, E. Frackowiak, Carbons and electrolytes for advanced supercapacitors, Adv. Mater. 26 (2014) 2219–2251, 2283.
[2] A. Vlad, A. Balducci, Supercapacitors: porous materials get energized, Nat. Mater. 16 (2017) 161–162.
[3] P.J. Hall, M. Mirzaeian, S.I. Fletcher, F.B. Sillars, A.J.R. Rennie, G.O. Shitta-Bey, G. Wilson, A. Cruden, R. Carter, Energy storage in electrochemical capacitors: designing functional materials to improve performance, Energy Environ. Sci. 3 (2010) 1238–1251.
[4] R. Kötz, M. Carlen, Principles and applications of electrochemical capacitors, Electrochim. Acta 45 (2000) 2483–2498.
[5] Y. Zhang, H. Feng, X.B. Wu, L.Z. Wang, A.Q. Zhang, T.C. Xia, H.C. Dong, X.F. Li, L.S. Zhang, Progress of electrochemical capacitor electrode materials: a review, Int. J. Hydrogen Energy 34 (2009) 4889–4899.
[6] K. Fic, M. Meller, E. Frackowiak, Strategies for enhancing the performance of carbon/carbon supercapacitors in aqueous electrolytes, Electrochim. Acta 128 (2014) 210–217.
[7] Q. Abbas, P. Ratajczak, P. Babuchowska, A. Le Comte, D. Belanger, T. Brousse, F. Beguin, Strategies to improve the performance of carbon/carbon capacitors in salt aqueous electrolytes, J. Electrochem. Soc. 162 (2015) A5148–A5157.
[8] A. Balducci, Electrolytes for high voltage electrochemical double layer capacitors: a perspective article, J. Power Sources 326 (2016) 534–540.
[9] K. Fic, M. Meller, J. Menzel, E. Frackowiak, Around the thermodynamic limitations of supercapacitors operating in aqueous electrolytes, Electrochim. Acta 206 (2016) 496–503.
[10] G.Z. Chen, Supercapacitor and supercapattery as emerging electrochemical energy stores, Int. Mater. Rev. 62 (2017) 173–202.
[11] Z. Wu, L. Li, J.M. Yan, X.B. Zhang, Materials design and system construction for conventional and new-concept supercapacitors, Adv. Sci. 4 (2017), 1600382.
[12] F. Bensebaa, Clean energy, Interface. Sci. Technol. 19 (2013) 279–383.
[13] J.R. Miller, A.F. Burke, Electrochemical capacitors: challenges and opportunities for real-world applications, Electrochem. Soc. Inter. 17 (2008) 53–57.
[14] F. Stoeckli, T.A. Centeno, Optimization of the characterization of porous carbons for supercapacitors, J. Mater. Chem. 1 (2013) 6865–6873.
[15] Y. Gogotsi, D. Guldi, R. McCreery, C.C. Hu, C. Merlet, F. Beguin, L. Hardwick, E. Frackowiak, J. Macpherson, A. Forse, G.Z. Chen, K. Holt, R. Dryfe, H. Kurig, S. Sharma, P.R. Unwin, T. Rabbow, W. Yu, F. Qiu, F. Juarez, C. Sole, B. Dyatkin, K. Stevenson, Y. Cao, N. Cousens, A. Noofeli, Carbon electrodes for energy storage: general discussion, Faraday Discuss 172 (2014) 239–260.
[16] M.F. Dupont, S.W. Donne, Separating faradaic and non-faradaic charge storage contributions in activated carbon electrochemical capacitors using electrochemical methods I. Step potential electrochemical spectroscopy, J. Electrochem. Soc. 162 (2015) A1246–A1254.
[17] A.C. Forse, C. Merlet, P.K. Allan, E.K. Humphreys, J.M. Griffin, M. Aslan, M. Zeiger, V. Presser, Y. Gogotsi, C.P. Grey, New insights into the structure of nanoporous carbons from NMR, Raman, and pair distribution function analysis, Chem. Mater. 27 (2015) 6848–6857.
[18] C. Zhong, Y. Deng, W. Hu, D. Sun, X. Han, J. Qiao, J. Zhang, Electrolytes for Electrochemical Supercapacitors, CRC Press, New York, 2016.
[19] L. Guan, L.P. Yu, G.Z. Chen, Capacitive and non-capacitive faradaic charge storage, Electrochim. Acta 206 (2016) 464–478.
[20] S. Yamazaki, T. Ito, Y. Murakumo, M. Naitou, T. Shimooka, M. Yamagata, M. Ishikawa, Hybrid capacitors utilizing halogen-based redox reactions at interface between carbon positive electrode and aqueous electrolytes, J. Power Sources 326 (2016) 580–586.
[21] J.Y. Hwang, M.F. El-Kady, M.P. Li, C.W. Lin, M. Kowal, X. Han, R.B. Kaner, Boosting the capacitance and voltage of aqueous supercapacitors via redox charge contribution from both electrode and electrolyte, Nano Today 15 (2017) 15–25.
[22] M. Mirzaeian, Q. Abbas, A. Ogwu, P. Hall, M. Goldin, M. Mirzaeian, H.F. Jirandehi, Electrode and electrolyte materials for electrochemical capacitors, Int. J. Hydrogen Energy 42 (2017) 25565–25587.
[23] M. He, K. Fic, E. Frąckowiak, P. Novák, E.J. Berg, Influence of aqueous electrolyte concentration on parasitic reactions in high-voltage electrochemical capacitors, Ener. Storage Mater. 5 (2016) 111–115.
[24] J. Krummacher, C. Schutter, L.H. Hess, A. Balducci, Non-aqueous electrolytes for electrochemical capacitors, Curr. Opin. Electroche. 9 (2018) 64–69.
[25] T. Sato, G. Masuda, K. Takagi, Electrochemical properties of novel ionic liquids for electric double layer capacitor applications, Electrochim. Acta 49 (2004) 3603–3611.
[26] M.P. Mousavi, B.E. Wilson, S. Kashefolgheta, E.L. Anderson, S. He, P. Buhlmann, A. Stein, Ionic liquids as electrolytes for electrochemical double-layer capacitors: Structures that optimize specific energy, ACS Appl. Mater. Interfaces 8 (2016) 3396–3406.
[27] K. Fic, A. Platek, J. Piwek, E. Frackowiak, Sustainable materials for electrochemical capacitors, Mater. Today 21 (2018) 437–454.
[28] K. Hiratsuka, Y. Sanada, T. Morimoto, K. Kurihara, Evaluation of activated carbon electrodes for electric double-layer capacitors using an organic electrolyte solution, Denki Kagaku 59 (1991) 607–613.
[29] C. Zhong, Y. Deng, W. Hu, J. Qiao, L. Zhang, J. Zhang, A review of electrolyte materials and compositions for electrochemical supercapacitors, Chem. Soc. Rev. 44 (2015) 7484–7539.
[30] Y. Wang, Y. Song, Y. Xia, Electrochemical capacitors: mechanism, materials, systems, characterization and applications, Chem. Soc. Rev. 45 (2016) 5925–5950.
[31] J. Wojciechowski, L. Kolanowski, A. Bund, G. Lota, The influence of current collector corrosion on the performance of electrochemical capacitors, J. Power Sources 368 (2017) 18–29.
[32] K. Fic, G. Lota, M. Meller, E. Frackowiak, Novel insight into neutral medium as electrolyte for high-voltage supercapacitors, Energy Environ. Sci. 5 (2012) 5842–5850.
[33] K. Fic, M. He, E.J. Berg, P. Novák, E. Frackowiak, Comparative operando study of degradation mechanisms in carbon-based electrochemical capacitors with Li

2 SO 4 and LiNO 3 electrolytes, Carbon 120 (2017) 281–293.
[34] L. Demarconnay, E. Raymundo-Pinero, F. Beguin, A symmetric carbon/carbon supercapacitor operating at 1.6 V by using a neutral aqueous solution, Electrochem. Commun. 12 (2010) 1275–1278.
[35] J.H. Chae, G.Z. Chen, 1.9 V aqueous carbon-carbon supercapacitors with unequal electrode capacitances, Electrochim. Acta 86 (2012) 248–254.
[36] S. Vaquero, J. Palma, M. Anderson, R. Marcilla, Mass-balancing of electrodes as a strategy to widen the operating voltage window of carbon/carbon supercapacitors in neutral aqueous electrolytes, Int. J. Electrochem. Sci. 8 (2013) 10293–10307.
[37] Q. Gao, Optimizing carbon/carbon supercapacitors in aqueous and organic electrolytes, Chemistry (2013) 1–155. Université d'Orléans, CRMD - Centre de Recherche sur la Matière Divisée.
[38] H.C. Chien, T.H. Wu, M. Rajkumar, C.C. Hu, Effects of buffer agents on hydrogen adsorption and desorption at/within activated carbon for the negative electrode of aqueous asymmetric supercapacitors, Electrochim. Acta 205 (2016) 1–7.
[39] E. Redondo, E. Goikolea, R. Mysyk, The decisive role of electrolyte concentration in the performance of aqueous chloride-based carbon/carbon supercapacitors with extended voltage window, Electrochim. Acta 221 (2016) 177–183.
[40] A. Slesinski, C. Matei-Ghimbeu, K. Fic, F. Beguin, E. Frackowiak, Self-buffered pH at carbon surfaces in aqueous supercapacitors, Carbon 129 (2018) 758–765.
[41] P. Azaïs, L. Duclaux, P. Florian, D. Massiot, M.-A. Lillo-Rodenas, A. Linares-Solano, J.-P. Peres, C. Jehoulet, F. Béguin, Causes of supercapacitors ageing in organic electrolyte, J. Power Sources 171 (2007) 1046–1053.
[42] O. Bohlen, J. Kowal, D.U. Sauer, Ageing behaviour of electrochemical double layer capacitors - Part II. Lifetime simulation model for dynamic applications, J. Power Sources 173 (2007) 626–632.
[43] O. Bohlen, J. Kowal, D.U. Sauer, Ageing behaviour of electrochemical double layer capacitors Part I. Experimental study and ageing model, J. Power Sources 172 (2007) 468–475.
[44] A.M. Bittner, M. Zhu, Y. Yang, H.F. Waibel, M. Konuma, U. Starke, C.J. Weber, Ageing of electrochemical double layer capacitors, J. Power Sources 203 (2012) 262–273.
[45] R. German, P. Venet, A. Sari, O. Briat, J.M. Vinassa, Interpretation of electrochemical double layer capacitors (Supercapacitors) floating ageing by multipore model, in: 2012 10th International Power & Energy Conference (IPEC), 2012, pp. 218–223.
[46] D. Weingarth, A. Foelske-Schmitz, R. Kötz, Cycle versus voltage hold – which is the better stability test for electrochemical double layer capacitors? J. Power Sources 225 (2013) 84–88.
[47] N. Omar, H. Gualous, J. Salminen, G. Mulder, A. Samba, Y. Firouz, M.A. Monem, P. Van den Bossche, J. Van Mierlo, Electrical double-layer capacitors: evaluation of ageing phenomena during cycle life testing, J. Appl. Electrochem. 44 (2014) 509–522.
[48] P. Ratajczak, K. Jurewicz, F. Beguin, Factors contributing to ageing of high voltage carbon/carbon supercapacitors in salt aqueous electrolyte, J. Appl. Electrochem. 44 (2014) 475–480.
[49] P. Ratajczak, K. Jurewicz, P. Skowron, Q. Abbas, F. Beguin, Effect of accelerated ageing on the performance of high voltage carbon/carbon electrochemical capacitors in salt aqueous electrolyte, Electrochim. Acta 130 (2014) 344–350.
[50] D. Torregrossa, K.E. Toghill, V. Amstutz, H.H. Girault, M. Paolone, Macroscopic Indicators of Fault Diagnosis and Ageing in Electrochemical Double Layer Capacitors, 2015, pp. 8–24.
[51] A. Balducci, D. Belanger, T. Brousse, J.W. Long, W. Sugimoto, A guideline for reporting performance metrics with electrochemical capacitors: from electrode materials to full devices, J. Electrochem. Soc. 164 (2017) A1487–A1488.
[52] J.P. Zheng, J. Huang, T.R. Jow, The limitations of energy density for electrochemical capacitors, J. Electrochem. Soc. 144 (1997) 2026–2031.
[53] T. Brousse, D. Bélanger, J.W. Long, To Be or not to Be pseudocapacitive? J. Electrochem. Soc. 162 (2015) A5185–A5189.
[54] J. Wang, S. Dong, B. Ding, Y. Wang, X. Hao, H. Dou, Y. Xia, X. Zhang, Pseudocapacitive Materials for Electrochemical Capacitors: from Rational Synthesis to Capacitance Optimization, 2017, pp. 71–90.
[55] W. Zuo, R. Li, C. Zhou, Y. Li, J. Xia, J. Liu, Battery-Supercapacitor hybrid devices: recent progress and future prospects, Adv. Sci. 4 (2017) 1600539.
[56] M.R. Lukatskaya, S. Kota, Z.F. Lin, M.Q. Zhao, N. Shpigel, M.D. Levi, J. Halim, P.L. Taberna, M. Barsoum, P. Simon, Y. Gogotsi, Ultra-high-rate pseudocapacitive energy storage in two-dimensional transition metal carbides, Nat. Ener. 2 (2017).
[57] Y. Gogotsi, R.M. Penner, Energy storage in nanomaterials - capacitive, pseudocapacitive, or battery-like? ACS Nano 12 (2018) 2081–2083.
[58] E. Frackowiak, M. Meller, J. Menzel, D. Gastol, K. Fic, Redox-active electrolyte for supercapacitor application, Faraday Discuss 172 (2014) 179–198.
[59] B. Akinwolemiwa, C. Peng, G.Z. Chen, Redox electrolytes in supercapacitors, J. Electrochem. Soc. 162 (2015) A5054–A5059.
[60] E. Mourad, L. Coustan, S.A. Freunberger, A. Mehdi, A. Vioux, F. Favier, O. Fontaine, Biredox ionic liquids: electrochemical investigation and impact of ion size on electron transfer, Electrochim. Acta 206 (2016) 513–523.
[61] P. Przygocki, Q. Abbas, F. Beguin, Capacitance enhancement of hybrid electrochemical capacitor with asymmetric carbon electrodes configuration in neutral aqueous electrolyte, Electrochim. Acta 269 (2018) 640–648.
[62] S.E. Chun, B. Evanko, X. Wang, D. Vonlanthen, X. Ji, G.D. Stucky, S.W. Boettcher, Design of aqueous redox-enhanced electrochemical capacitors with high specific energies and slow self-discharge, Nat. Commun. 6 (2015) 7818.
[63] K. Fic, M. Meller, E. Frackowiak, Interfacial redox phenomena for enhanced aqueous supercapacitors, J. Electrochem. Soc. 162 (2015) A5140–A5147.
[64] X. Wang, R.S. Chandrabose, S.E. Chun, T. Zhang, B. Evanko, Z. Jian, S.W. Boettcher, G.D. Stucky, X. Ji, High energy density aqueous electrochemical capacitors with a KI-KOH electrolyte, ACS Appl. Mater. Interfaces 7 (2015) 19978–19985.
[65] M. Meller, J. Menzel, K. Fic, D. Gastol, E. Frackowiak, Electrochemical capacitors as attractive power sources, Solid State Ionics 265 (2014) 61–67.
[66] P. Przygocki, Q. Abbas, P. Babuchowska, F. Beguin, Confinement of iodides in carbon porosity to prevent from positive electrode oxidation in high voltage aqueous hybrid electrochemical capacitors, Carbon 125 (2017) 391–400.
[67] J. Menzel, K. Fic, E. Frackowiak, Hybrid aqueous capacitors with improved energy/power performance, Prog. Nat. Sci-Mater. 25 (2015) 642–649.
[68] Q. Abbas, D. Pajak, E. Frackowiak, F. Beguin, Effect of binder on the performance of carbon/carbon symmetric capacitors in salt aqueous electrolyte, Electrochim. Acta 140 (2014) 132–138.
[69] J. Jagiello, J.P. Olivier, A simple two-dimensional NLDFT model of gas adsorption in finite carbon pores. Application to pore structure analysis, J. Phys. Chem. C 113 (2009) 19382–19385.
[70] J. Jagiello, J.P. Olivier, Carbon slit pore model incorporating surface energetical heterogeneity and geometrical corrugation, Adsorption-J. Int. Adsorp. Soc. 19 (2013) 777–783.
[71] J. Jagiello, J.P. Olivier, 2D-NLDFT adsorption models for carbon slit-shaped pores with surface energetical heterogeneity and geometrical corrugation, Carbon 55 (2013) 70–80.
[72] M. Meller, K. Fic, J. Menzel, E. Frackowiak, Electrode/electrolyte interface with various redox couples, ECS Transactions 61 (2014) 1–8.
[73] J. Menzel, K. Fic, M. Meller, E. Frackowiak, The effect of halide ion concentration on capacitor performance, J. Appl. Electrochem. 44 (2014) 439–445.
[74] Q. Abbas, F. Beguin, Influence of the iodide/iodine redox system on the self-discharge of AC/AC electrochemical capacitors in salt aqueous electrolyte, Prog. Nat. Sci-Mater. 25 (2015) 622–630.
[75] Q. Abbas, P. Babuchowska, E. Frckowiak, F. Beguin, Sustainable AC/AC hybrid electrochemical capacitors in aqueous electrolyte approaching the performance of organic systems, J. Power Sources 326 (2016) 652–659.